

Reactivities of American, Chinese and Estonian oil shale semi-cokes and Argonne premium coal chars under oxy-fuel combustion conditions

Chris Culin^(a), Kevin Tente^(a), Alar Konist^(a,b), Birgit Maaten^(b),
Lauri Loo^(b), Eric Suuberg^(a), Indrek Külaots^{(a)*}

^(a) School of Engineering, Brown University, 184 Hope St., Providence, RI, USA, 02912

^(b) Department of Energy Technology, Tallinn University of Technology, Ehitajate tee 5, 19086 Tallinn, Estonia

Abstract. *Oil shales of various rank and origin from China, Estonia and the United States are investigated and their oxidation reactivities under simulated oxy-fuel combustion conditions, in air, and in 100% CO₂ atmospheres explored. Independent of rank and origin, as the oil shale pyrolysis temperature increases, the oil shale semi-coke oxidation reactivity decreases. The oxidation reactivities in air and in simulated oxy-fuel oxidation atmospheres for all of the oil shale semi-cokes tested are more or less the same. Oil shale semi-coke oxidation reaction activation energies in an air atmosphere are similar to the activation energies obtained under the simulated oxy-fuel conditions. These findings are useful for optimizing retrofit of current oil shale-fired systems to oxy-fuel combustion conditions, particularly if they are to be fired with oil shale semi-coke from retorting processes.*

Keywords: *oil shale semi-coke, coal chars, pyrolysis, oxidation reactivity, oxy-fuel combustion, activation energy.*

1. Introduction

Oil shale, a fine-grained sedimentary rock, is found in vast deposits in the United States and worldwide [1–3]. It often contains a large amount of kerogen, which can be converted into oil by thermal degradation or “retorting”, a process from which a primary byproduct is carbon rich semi-coke [4, 5]. This old-fashioned retorting process extracts as oil only a portion of the energy value of the resource and leaves behind some of the potential energy content as a carbonaceous component in the semi-coke. In addition to its use as an oil source, oil shale, if rich enough in organic content, may be directly fired in boilers. Estonia is one of the few countries in the world that utilizes oil

shale as a fuel source for electricity generation. According to the U.S. Energy Information Administration 2016 data in Estonia, out of a total of 12 billion kWh electrical energy generation, 85.8% originates from thermal power plants directly firing oil shale [6].

Large amounts of CO₂ are emitted from Estonian thermal power plants, operating on pulverized and fluidized bed combustion technologies involving oil shale. Conventional pulverized oil shale combustors generate large volumes of diluted CO₂ in combustion flue gases, originating both from oil shale kerogen oxidation as well as from decomposition of the accompanying carbonate minerals, calcite and dolomite. The amounts of these carbonates are large in oil shales, with values as high as 1/3 by mass. As great an incentive as there might be to perform CO₂ capture in such a system, because CO₂ concentrations in the flue gas are still low, typically less than 15% [7], these conventional combustion systems offer little opportunity for CO₂ capture and sequestration.

During the past decade, oil shale has been successfully used in fluidized bed combustors, leading to higher energy conversion efficiencies and lower emissions [8, 9]. Because of the lower operating temperatures of such systems, carbonate decomposition is not as great. Standard fluidized combustion systems, however, neither support the removal of CO₂ nor lower NO_x emissions without costly modifications. Recent objectives to further reduce the emissions from power generation combustion units, which are operated on oil shale or any other lower grade fuel, have led investigators to explore retrofitting the existing pulverized systems for oxy-fuel combustion [10, 11] since this will have a minimal impact on the boiler-turbine steam cycle.

Oxy-fuel combustion is a promising alternative technology for coal combustion, as it enables carbon capture and storage and leads to lower SO₂ and NO_x emissions, while maintaining high overall efficiency [12, 13]. In oxy-fuel combustion, atmospheres of pure oxygen and recycled flue gas (mostly CO₂) are used as the oxidizing medium, rather than atmospheric air. The oxy-fuel combustion technique typically involves cryogenic separation of air to produce oxygen and nitrogen, prior to the use of the oxygen in the combustion process (oxygen purity should be at least 95% [14, 15]). Prior to combustion, oxygen is mixed with partially recycled CO₂ at concentrations typically around 30% of O₂ and 70% of CO₂ [13]. The resulting flue gases consist entirely of water vapor and CO₂, which are readily separated, leaving CO₂ ready for sequestration [16–18]. In addition, in oxy-fuel systems, NO_x emissions are significantly reduced because of the removal of nitrogen from the air and due to removal of the thermal NO_x pathway [19, 20]. According to Normann et al. [21], preliminary efforts have led to a reduction of around 65% of the NO_x emission (per unit of fuel supplied) during oxy-fuel combustion compared to air-combustion, utilizing technology designed for air firing [21]. Oxy-fuel systems based on coal are reported to feature high overall thermal process efficiency, the ability fully to remove concentrated CO₂ from the flue gases

and to reduce the total volume of combustion gases, up to 80 vol% [13, 21]. As shown by McCauley et al. [22], the results of pilot-scale bituminous and sub-bituminous coal combustion trials in oxy-fuel units have been promising. The first successful pilot-scale 20 kW oxy-fuel combustion results using oil shale from Jordan were presented by Al-Makhadmeh et al. [19]. That study reported that the SO₂ and NO_x emissions were approximately 30% lower compared to results obtained by combustion of the same oil shale in air.

Oxy-fuel combustion occurs in CO₂ rich oxygen/carbon dioxide mixtures, which is quite a different combustion environment if compared to the combustion in the conventional air atmosphere. The high char oxidation rate is still desired since it helps to keep boiler size small. Although bituminous coal reactivity under oxy-fuel combustion conditions has been widely investigated, there have been only a few studies on oil shale oxidation reactivity in an oxy-fuel combustion environment and some of the results have led to unclear conclusions regarding the behavior of these materials.

Prior research with bituminous coals in oxy-fuel conditions has indicated a significant contribution from CO₂-char reactivity at temperatures about 1030 K [23]. Another study [13] has reported that coal char burnout is slightly higher in the oxy-fuel gas environment than in air under comparable conditions. As a result of the contribution of the oil shale char-CO₂ reaction, Konist et al. [20] showed that oil shale oxy-fuel combustion at elevated CO₂ levels had a significant influence on the extent of carbonate decomposition and therefore on the SO₂-binding properties of the residual mineral matter. Meriste et al. [24] have found that Estonian oil shale combustion proceeds with lower apparent activation energies in oxy-fuel simulated gas environments compared to activation energies obtained in air.

To our knowledge there have been no systematic investigations of oil shale oxidation reactivity under oxy-fuel combustion conditions for oil shales obtained from the many different sources of oil shale in the world. Oil shale is a heterogenous material, and the compositions of oil shales from different continents show some differences. Therefore, our study aims to provide comprehensive oxidation reactivity results for oil shales obtained from several very distinct sources. These oil shale reactivity results will be compared with those on Argonne premium coal samples [25] under oxy-fuel combustion conditions.

2. Experimental

2.1. Materials tested

A total of four oil shale samples were used in this research. Two of the samples originated from Maoming mine, Guangdong Province, southwest China with local classifications, or rank, of A and C (below referred to as “Chinese M-A” and “Chinese M-C”). One sample was from the Aidu mine in northeast

Estonia (referred to as “Estonian”) and one sample was from the Green River Formation in Colorado, USA (referred to as “Colorado”). All oil shale samples were ground and sieved prior to use, and particle fractions from 45 to 75 μm in diameter were selected for use.

For comparison purposes, three standard coal samples – Illinois#6 (high volatile class C bituminous coal), Pittsburgh#8 (high volatile Class A bituminous coal) and Wyodak-Anderson (subbituminous coal) from the Argonne National Laboratory premium coal sample bank [25] were also investigated. Ampoules containing 5 grams of each 100-mesh (up to 150 μm) coal were purchased from Argonne National Laboratory, Argonne, IL, and were pyrolyzed with no further preparation.

2.2. Oil shale and coal pyrolysis

Oil shale semi-cokes and coal chars were prepared in the same way. Approximately 3 grams of oil shale or coal sample was placed into a porcelain crucible which was inserted into a laboratory tube furnace. A continuous 300 ml/min helium gas flow purged the tube furnace of any oxygen. Oil shales were heated at set furnace heating rate of 20 K/min to either of two target temperatures of 500 °C and 1000 °C, at which the samples were then kept for one hour. Samples were cooled down to room temperature while maintaining the 300 ml/min helium gas purge flow. The mass loss during the 500 °C oil shale pyrolysis experiment was attributed mostly to the removal of kerogen and water, while the mass loss from oil shale heated at 1000 °C could be attributed to the removal of water, kerogen and the decomposition of carbonate minerals. For three coal samples the same pyrolysis procedure was applied as for oil shales except that only a 1000 °C pyrolysis temperature was explored. The solid products obtained after pyrolysis experiments were called oil shale semi-cokes and coal chars. Fisher Assay oil yield, in units of gallons of oil per ton of oil shale (GPT), was estimated as described by Cook [26].

2.3. Oil shale semi-coke and coal char organic matter contents and reactivity tests

A Mettler Toledo thermogravimetric analyzer and differential scanning calorimeter (TGA/DSC-1) was used to determine the oil shale semi-coke and coal char organic matter and mineral contents. In these experiments, approximately 15 to 20 mg of semi-coke or coal char sample was placed into a 150 μl aluminum crucible, which was inserted into the TGA-DSC-1. The samples were heated at a rate of 30 K/min to 120 °C under a 100 ml/min air flow and held at this temperature for 20 min to remove physically absorbed water. After this water removal, the oil shale semi-cokes and coal char samples were heated at a heating rate of 20 K/min to 600 °C and held for 35 minutes at this temperature to determine the sample combustible (organic) contents.

The 600 °C air oxidation temperature in the TGA experiments for the 500 °C target temperature pyrolyzed oil shales has been carefully selected. At temperatures above 620 °C, decomposition of carbonate minerals contributes significantly to the observed mass loss from oil shale semi-cokes. Such mineral decomposition related mass loss should not be included when determining the organic carbon content in oil shale semi-cokes [27, 28]. Oil shale mineral carbonate decomposition in the TGA experiments was not a concern with oil shale samples pyrolyzed at 1000 °C, because the carbonate decomposition reactions had likely gone to completion during pyrolysis, however, oil shale samples pyrolyzed at 500 °C would still contain intact carbonate mineral matter. Therefore, care needed to be taken in examining the effect of oxidation temperatures for samples pyrolyzed at the lower temperature.

Oil shale semi-coke and coal char reactivity tests were performed with the same Mettler Toledo TGA/DSC-1 instrument. In each reactivity experiment, approximately 10 mg of sample was placed into a 150 µL aluminum crucible. Samples were heated at a heating rate of 20 K/min to the temperature at which oxidation started in a 100 ml/min total flowing gas environment. Several different gas environments were examined: 1) dry commercial grade air, 2) high purity commercial grade CO₂, and 3) in order to simulate oxy-fuel oxidation conditions 25 vol% O₂ and 75 vol% CO₂. Once measurable reactivity was observed, temperatures were increased in a stepwise manner, in order to determine the kinetic parameters for oxidation of oil shale semi-cokes and coal chars. The oxidation reaction rate data were recorded for one minute at each isothermal temperature step. The instrument heating rate between the isothermal oxidation rate recording steps was 10 K/min.

The critical temperature, as defined by Charpenay et al. [29], is the temperature at which an organic char mass loss rate is equal to 0.065 min⁻¹. This critical temperature approach was used to determine a standardized sample reactivity measure. The lower the temperature at which the rate reaches the 0.065 min⁻¹ criterion, the higher the reactivity of the sample [30]. Critical temperatures of coal and oil shale chars were found in the TGA using a non-isothermal method, applying a standard heating rate of 20 K/min. Recorded oxidation rates (mg/min) were in all cases normalized by the initial organic carbon contents in oil shale semi-cokes or chars, as determined from the 600 °C burnout experiments described above.

2.4. Semi-coke and coal char oxidation model

There are several oxidation models that have been applied to oil shales (as distinct from the semi-cokes of these oil shales). Some involve three, some four, and a few even as many as six distinct stages. The three-step oil shale oxidation model leaves out the mineral portion (carbonate) decomposition step, but includes water evaporation, devolatilization/volatiles combustion and finally the organic char oxidation step [31]. The earlier studies of oil shale

semi-coke oxidation have established that the overall rate-limiting step in oil shale oxidation is the organic char oxidation step. In a practical process, this step determines the overall residence time required for oil shale oxidation. Here, we focus only on that semi-coke oxidation step. Therefore, we express oil shale semi-coke global oxidation kinetics as [32]:

$$r = \frac{dx}{dt} = k(1-x)P^n, \quad (1)$$

where k is the rate constant, P is the partial pressure of oxygen, n is the oxygen-dependent reaction order, and x is the fractional extent of conversion of the semi-coke at any time, t . The extent of conversion can be obtained from the experimental data as follows:

$$x = \frac{m_i - m_t}{m_i - m_c}, \quad (2)$$

where m_i is the initial mass of the semi-coke (after drying), m_t is the mass at time t , and m_c is the mass of the semi-coke following complete loss of the organic char portion of the semi-coke.

The rate constant, k , can be represented by the Arrhenius equation involving the activation energy, E_a , and the pre-exponential factor, A :

$$k = A \exp\left(-\frac{E_a}{RT}\right), \quad (3)$$

where R is the universal gas constant and T the absolute temperature. The activation energies were determined in temperature ranges within which reaction rate itself, rather than diffusion, was limiting.

3. Results and discussion

The oil shales investigated had Fisher Assay oil yields ranging from 38 to 77 GPT, which are fairly typical of oil shales of commercial interest [27]. The Estonian oil shale showed the highest oil yield, while the lowest oil yield was obtained from the Chinese M-C oil shale sample. Depending on the origin of the oil shale, or its rank, and the pyrolysis temperature, the organic char content of oil shale semi-cokes ranged from 2.1 wt% to 19.3 wt% (see Table 1 for 1000 °C pyrolysis data and Table 2 for 500 °C pyrolysis data).

Table 1. The organic char contents, critical temperatures, activation energies and pre-exponential factors for 1000 °C pyrolyzed oil shales oxidized in air, in 100% CO₂ and in simulated oxy-fuel (75 vol% CO₂/25 vol% O₂) combustion atmospheres

Oil shale semi-coke	Organic char, wt%	Critical temperature, °C	Activation energy, kJ/mol	Pre-exponential factor, s ⁻¹
Chinese M-A, in air	12.0	534	193 ± 6	9.8E + 11
Chinese M-A, in CO ₂		946	293 ± 19	3.5E + 11
Chinese M-A, in oxy-fuel		529	198 ± 3	6.1E + 11
Chinese M-C, in air	4.2	521	144 ± 10	1.2E + 08
Chinese M-C, in CO ₂		892	222 ± 8	5.3E + 09
Chinese M-C, in oxy-fuel		503	224 ± 6	1.4E + 14
Estonian, in air	7.6	503	107 ± 4	5.2E + 06
Estonian, in CO ₂		828	293 ± 5	8.0E + 04
Estonian, in oxy-fuel		498	141 ± 8	1.1E + 19
Colorado, in air	2.1	465	121 ± 2	1.9E + 07
Colorado, in CO ₂		879	282 ± 14	1.3E + 16
Colorado, in oxy-fuel		467	130 ± 3	5.8E + 07

Table 2. The organic char contents, critical temperatures, activation energies and pre-exponential factors for the 500 °C pyrolyzed oil shales oxidized in air and in simulated oxy-fuel (75 vol% CO₂/25 vol% O₂) atmospheres

Oil shale semi-coke	Organic char, wt%	Critical temperature, °C	Activation energy, kJ/mol	Pre-exponential factor, s ⁻¹
Chinese M-A, in air	7.6	347	125.9 ± 1.9	1.2E + 09
Chinese M-A, in oxy-fuel		389	114 ± 2	5.4E + 07
Chinese M-C, in air	9.7	367	115.8 ± 2.3	7.2E + 07
Chinese M-C, oxy-fuel		365	108 ± 4	3.6E + 07
Estonian, in air	19.3	378	130.3 ± 5.0	1.1E + 09
Estonian, in oxy-fuel		356	100 ± 1	9.2E + 06
Colorado, in air	6.1	371	106.9 ± 5.0	3.7E + 05
Colorado, in oxy-fuel		382	141 ± 1	1.1E + 10

These results agree well with previously published values [33]. As addressed in the study by Kūlaots et al. [27], the difficulty in measuring the true organic content in semi-cokes is mostly associated with the high contents of carbonate minerals (calcite, dolomite and ankerite). Any oil shale semi-cokes which are pyrolyzed at temperatures below about 850 °C (such as the 500 °C samples examined here) still might contain some portion of undecomposed carbonates, which could decompose during the semi-coke oxidation experiments [28]. The presence of undecomposed carbonates in oil shale semi-cokes could lead to the overestimation of organic char content in an oil shale semi-coke. Therefore, we have taken great care while oxidizing our 500 °C pyrolyzed samples and avoided going much above this temperature in the corresponding oxidation experiments.

As seen from the results presented in Tables 1 and 2, the organic char contents of semi-cokes decrease as the pyrolysis temperature increases. This trend is expected since the organic content in lower temperature semi-cokes is believed to still possess some hydrocarbon character [27]. This is the reason why the organic portion in oil shale semi-cokes should not be referred to as “carbon content” since it can still be somewhat hydrocarbon-like in nature.

As shown in Table 3, the carbon content in the Argonne premium 1000 °C pyrolyzed coal chars ranges from 72.2 wt% up to 81.7 wt%, and is much higher than the organic matter content in oil shale semi-cokes. It is important to note that these are not so-called “fixed carbon” values in a typical solid fuel proximate analysis, because they are here reported on a mineral-matter containing basis, so as to be comparable to the basis for reporting the oil shale semi-coke organic char.

Table 3. The organic char contents, critical temperatures for Argonne premium coals pyrolyzed at 1000 °C and oxidized in air, in 100% CO₂ and in the simulated oxy-fuel atmosphere (75 vol% CO₂/25 vol% O₂)

Argonne premium coal char	Organic char, wt%	Critical temperature, °C
Wyodak, in air	78.6	462
Wyodak, in CO ₂		949
Wyodak, in oxy-fuel		544
Pittsburgh, in air	81.7	574
Pittsburgh, in CO ₂		1093
Pittsburgh, in oxy-fuel		586
Illinois, in air	72.2	570
Illinois, in CO ₂		1095
Illinois, in oxy-fuel		595

Figure 1a shows the oxidation curves of Chinese M-A, 1000 °C oil shale semi-coke in air, in CO₂ and under simulated oxy-fuel oxidation (75 vol% CO₂ and 25 vol% O₂) atmospheres. In the air and the simulated oxy-fuel atmosphere, the oxidation of Chinese M-A, 1000 °C oil-shale semi-coke takes place in the same temperature range between 450 °C and 650 °C, while in a pure CO₂ atmosphere as expected the oxidation is slower and it begins at 850 °C. The small difference between the curves below about 100 °C just reflects a small difference in the moisture contents between the starting samples and is of no significance.

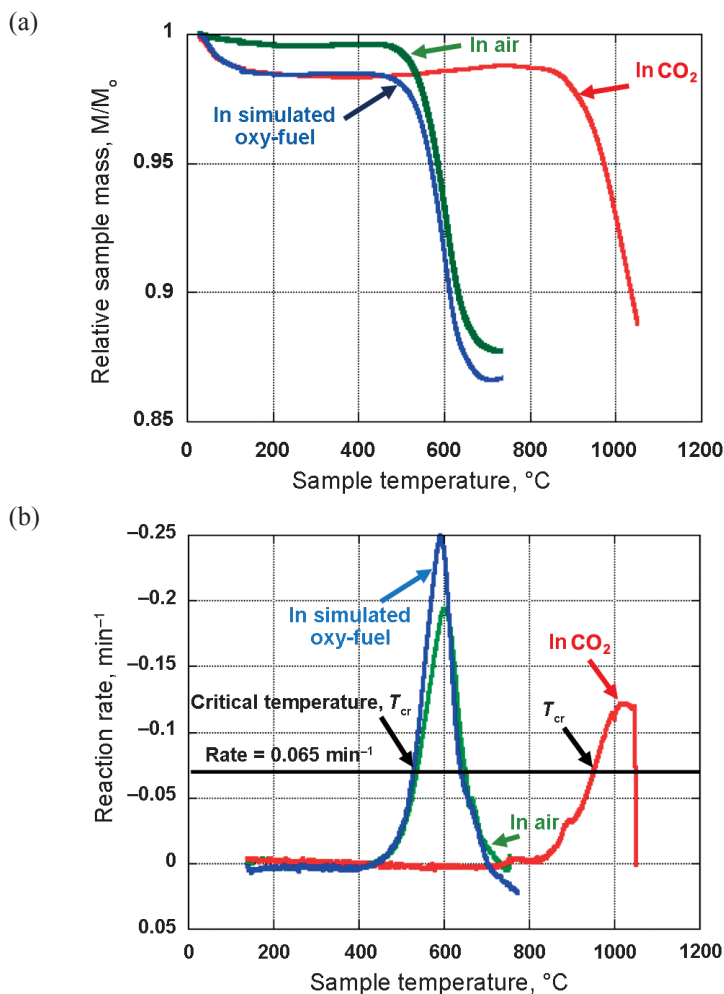


Fig. 1. (a) The 1000 °C pyrolyzed Chinese M-A oil shale relative oxidation mass loss in the air, in 100% CO₂ and in simulated oxy-fuel (75 vol% CO₂ and 25 vol% O₂) atmospheres; (b) the reaction rates and critical temperatures of the 1000 °C pyrolyzed Chinese M-A oil shale oxidation in air, in 100% CO₂ and in simulated oxy-fuel (75 vol% CO₂ and 25 vol% O₂) atmospheres.

It is evident that high temperatures are needed for semi-coke char oxidation in a pure CO₂ environment compared with oxidation in an air atmosphere. In fact, the results from Figure 1a show that the burnout in the simulated oxy-fuel environments is entirely completed at temperatures below which the CO₂ could make any significant contribution to the oxidation. This result merely reflects the nature of the present experiment, in which the sample was progressively heated; if this oil shale semi-coke had instead suddenly been introduced into an environment at a temperature above 850 °C, then both reaction pathways might well have contributed to the burnout.

Similar mass loss curves were recorded for all the other oil shale semi-cokes pyrolyzed at 500 °C and 1000 °C. The mass loss curves (such as that in Fig. 1a) were used to calculate the oxidation reaction rates and critical temperatures. Figure 1b shows the same oxidation data as curves of rate as a function of sample temperature. As noted in Figure 1b, the critical temperature in CO₂ for the Chinese M-A, 1000 °C oil shale semi-coke (946 °C) is significantly higher than the critical temperature observed in the air (534 °C) and in a simulated oxy-fuel atmosphere (529 °C), consistent with what is generally known regarding the relative rates of gasification in oxygen and CO₂. Also, it is unlikely that the small difference between the air and simulated oxy-fuel values can be regarded as significant.

The critical temperatures for 1000 °C pyrolyzed oil shale semi-cokes oxidized in air, in pure CO₂ and in simulated oxy-fuel atmospheres are summarized in Table 1. Table 2 provides the critical temperatures for 500 °C pyrolyzed oil shale semi-cokes oxidized in air and in the simulated oxy-fuel atmosphere. Independent of the oil shale origin and rank, the critical temperatures of 500 °C pyrolyzed oil shale semi-cokes (Table 2) are much lower than the values for the 1000 °C pyrolyzed samples in Table 1, indicating higher oxidation reactivity of the lower temperature prepared samples. This cannot be regarded as surprising since it is known that the char reactivities generally drop with increasing temperatures of heat treatment due to the thermal annealing effect [34]. At 1000 °C (Table 1) the oil shale semi-coke organic matter has lost its hydrocarbon nature and perhaps porosity [35] needed for higher oxidation rate, and therefore the 1000 °C pyrolyzed oil shale semi-cokes exhibit lower reactivity compared to the 500 °C pyrolyzed oil shales. There is no obvious trend with the oil shale rank or origin in terms of the oxidation reactivity in air.

As expected, critical temperatures in a pure CO₂ gas environment are much higher than those obtained in an air atmosphere (see Table 1). The critical temperatures of the 1000 °C pyrolyzed oil shale semi-cokes and oxidized in CO₂ range from 828 °C to 946 °C.

Even though one might expect lower critical temperatures under oxy-fuel combustion conditions as compared with air atmospheres, the present experiments would not reveal such differences, since as discussed in connection with Figure 1a, the reaction processes go to completion before

a temperature can be reached at which the CO_2 reactions can contribute. Thus, in considering the results for the 500 °C semi-cokes in Table 2 and the 1000 °C semi-cokes in Table 1, the oxy-fuel simulated gas environment critical temperatures are not significantly different from those obtained in air. Also, the oxidation reactivities for all oil shale semi-cokes tested in air and in the simulated oxy-fuel atmosphere are quite similar, though in the case of the 1000 °C samples the Estonian and Colorado oil shales seem to give slightly more reactive semi-cokes.

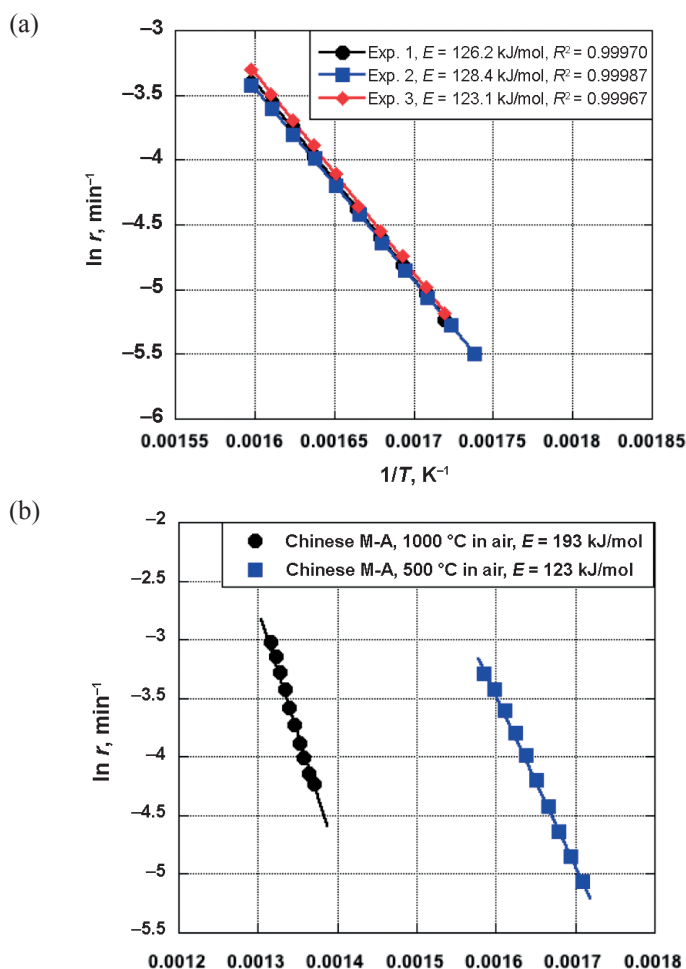


Fig. 2. (a) The 500 °C pyrolyzed Chinese M-A oil shale oxidation in air. The results of the three oxidation experiments are shown. The average activation energy, $E = 125.9$ kJ/mol is recorded in Table 2. (b) The 500 °C and 1000 °C pyrolyzed Chinese M-A oil shale sample oxidation in the air atmosphere. Notice, the 500 °C pyrolyzed Chinese M-A oil shale sample is much more reactive and has, therefore, lower activation energy.

If oxidized in the air atmosphere, the Argonne premium coal char (after 1000 °C pyrolysis) critical temperatures range from 462 °C to 570 °C (see the results in Table 3). These oxidation reactivities are comparable to those for the 1000 °C oil shale semi-cokes. As expected, the sub-bituminous coal char (Wyodak-Anderson) gives a more reactive char (with lower critical temperature) compared to the bituminous coals (Illinois#6 and Pittsburgh#8). The values for the coal chars bracket those for the oil shale semi-cokes, so in terms of intrinsic burnout kinetics, the oil shale semi-cokes would then not be expected to behave much differently than do the coal chars. What is interesting is that the coal chars oxidized in simulated oxy-fuel atmospheres show consistently higher critical temperatures (less reactive) compared to the oxidation critical temperatures obtained in air atmospheres. This was not the case with oil shale semi-cokes, and the reasons for this are not immediately apparent.

The activation energies and pre-exponential factors for the various oxidation processes involving the oil shale semi-cokes are provided in Tables 1 and 2 and Figures 2 to 3. These parameters are obtained using the isothermal method described above, rather than from the non-isothermal results. Figure 2a shows the results of 500 °C Chinese M-A oil shale semi-coke gasification in air. The results of three consecutive experiments with the same semi-coke sample are shown in this figure. The average activation energy, $E = 125.9$ kJ/mol calculated from the rate data of three experiments is given in Table 2.

All the oil shale semi-coke Arrhenius analysis results were reported from data obtained in double or triplicate. Figure 2b shows the 500 °C and 1000 °C temperature pyrolyzed Chinese M-A oil shale semi-coke gasification in air. As seen, the 500 °C degree semi-coke is much more reactive and has lower activation energy respectively. The 1000 °C semi-coke has gone through thermal annealing and therefore, is less reactive in any gas atmosphere. Figure 3a shows the results for the 500 °C temperature pyrolyzed Colorado, Chinese M-A, Chinese M-C and Estonian oil shale semi-cokes all gasified in simulated oxy-fuel conditions. The activation energies recorded are within 100 and 140 kJ/mol, with Colorado oil shale semi-coke having the highest activation energy. The activation energies of 1000 °C temperature pyrolyzed Chinese M-A oil shale semi-cokes gasified in simulated oxy-fuel conditions, in air and in a pure CO₂ atmosphere are shown in Figure 3b. As evidenced, the gasification rates and activation energies of this oil shale semi-coke are more or less the same in air and in simulated oxy-fuel conditions.

Overall, the activation energies obtained for oil shale semi-cokes pyrolyzed at 1000 °C in the air atmosphere range from 144 to 193 kJ/mol, while in oxy-fuel oxidation conditions the activation energies range from 130 to 224 kJ/mol. Therefore, our results suggest that overall the oil shale semi-coke activation energies are more or less the same when gasified in a simulated oxy-fuel or in an air atmosphere. Meriste et al. [24] have studied an oil shale semi-coke combustion under similar conditions, but reported some very different values

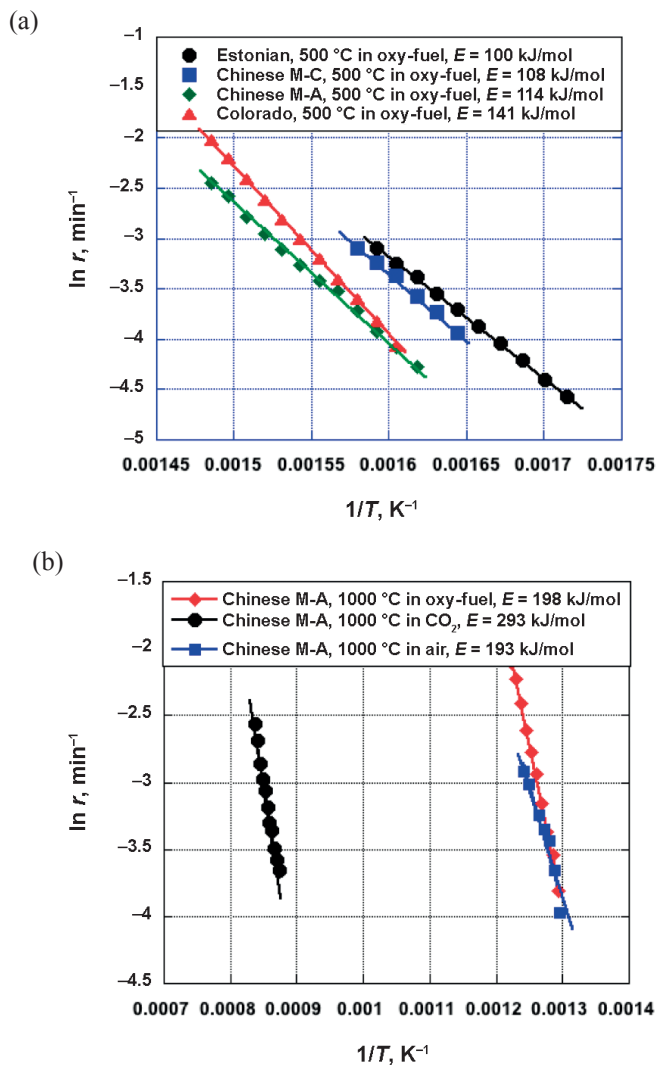


Fig. 3. (a) The 500 °C pyrolyzed Colorado, Chinese M-A, Chinese M-C and Estonian oil shales oxidized in simulated oxy-fuel conditions. Notice, the activation energies recorded are between 100 and 140 kJ/mol. (b) The 1000 °C pyrolyzed Chinese M-A oil shale oxidized in simulated oxy-fuel conditions, in air and in a pure CO_2 atmosphere. Notice, the rates and activation energies of oil shale semi-cokes are more or less the same in air and in simulated oxy-fuel conditions.

of activation energy, tending to be much lower than those cited here. But it is critical to note the different conditions that were examined in the two studies. The activation energies obtained in this study were for pyrolyzed samples and were obtained under reaction rate-controlled Zone I conditions [35]. As shown

by Külaots et al. [35], the activation energies for higher temperatures of the Arrhenius plot provide internal pore diffusion-controlled (Zone II conditions) rate data in which case the observed activation energy becomes approximately half of the true activation energy. As may be seen from Figure 2, the oxidation of 500 °C semi-coke chars was only examined up to 400 °C, and those of 1000 °C pyrolyzed chars up to 500 °C, and the results in Figure 3 involved only slightly higher temperatures. In contrast with this, the study by Meriste et al. [24] involved raw (unpyrolyzed) samples which would have superimposed a significant amount of pyrolysis on top of the oxidation reactions (their FTIR spectra showed significant evolution of hydrocarbons, which would have been gone in the present study, given the different experimental conditions). Meriste et al. also reported composite activation energies using the Friedman method (which is also described by Zhang et al. [36]). This would, of course, combine the results of very different mechanistic steps into one composite activation energy, which varies with conversion, as the results obtained by Meriste et al. [24] have shown. Another key difference between our results and those from Meriste et al. is that the activation energies they reported for higher degrees of organic material burnout were obtained at high enough temperatures that a transition to internal pore diffusion-controlled Zone II is possible [35]. This would inevitably lead to lower apparent activation energies for the char burnout that was taking place at the higher burnouts. The apparently significantly lower activation energies for burnout under oxy-fuel conditions reported by Meriste et al. [24] are then almost surely due to the fact that they examined the kinetics under conditions where different reactions would overlap under different mass transfer limitation conditions, which is known to lead to observations of low overall activation energy. It may be argued that the experiments by Meriste et al. are more representative of the history that the particles will experience under real combustion conditions, in that they were not pre-pyrolyzed (though the heating rates used in those experiments were still far below those of practical interest). On the other hand, the experiments in the present paper have sought to separate the different steps in the combustion to show more definitively what the intrinsic kinetics of the key char burnout step might be.

4. Conclusions

The kinetics of char burnout of different oil shale semi-cokes has been studied. The Fisher Assay oil yields from the tested oil shales ranged from 38 to 78 GPT. The organic char content of the studied oil shale semi-cokes ranged from 2.1 up to 17.8%. The organic char content decreased with an increase of pyrolysis temperature and any volatile matter was mostly lost by 1000 °C. The oxidation reaction rates characterized by the so-called “critical temperature” ranged from 350 °C to 500 °C and these values were independent of the

oil shale rank and origin. The activation energies for the oxidation of these samples were similar to those that have been reported for other chars, such as those from coals. The oxidation rates recorded for all oil shale semi-cokes tested were more or less similar in simulated oxy-fuel and air atmospheres. There seemed to be no contribution of CO₂ presence in the simulated oxy-fuel atmosphere to the oxidation rate given the nature of the slow heating experiments conducted here. The activation energies for all 500 °C oil shale semi-cokes oxidized in air and in the simulated oxy-fuel atmosphere ranged from 100 kJ/mol up to 141 kJ/mol. These findings are useful for the design of current oil shale-fired systems to oxy-fuel combustion conditions, particularly if they are to be fired with semi-coke from retorting processes.

REFERENCES

1. Duncan, D. C., Swanson, V. E. *Organic-Rich Shale of the United States and World Land Areas*. Geological Survey Circular 523, Washington, 1965.
2. Dyni, J. R. Geology and resources of some world oil-shale deposits. *Oil Shale*, 2003, **20**(3), 193–252.
3. Dyni, J. R. *Geology and Resources of Some World Oil-Shale Deposits*. Scientific Investigation Report 2005-5294. U.S. Geological Survey, Reston, Virginia, 2006.
4. Han, X., Kulaots, I., Jiang, X., Suuberg, E. M. Review of oil shale semicoke and its combustion utilization. *Fuel*, 2014, **126**, 143–161.
5. Sennoune, M., Salvador, S., Quintard, M. Reducing CO₂ emissions from oil shale semicoke smoldering combustion by varying the carbonate and fixed carbon contents. *Combust. Flame*, 2011, **158**(11), 2272–2282.
6. U.S. Department of Energy, E.I.A., *International Energy Statistics, Estonia*. 2016.
7. Figueroa, J. D., Fout, T., Plasynski, S., McIlvried, H., Srivastava, R. D. Advances in CO₂ capture technology – The U.S. Department of Energy’s Carbon Sequestration Program. *Int. J. Greenh. Gas Con.*, 2008, **2**(1), 9–20.
8. Jiang, X. M., Han, X. X., Cui, Z. G. Progress and recent utilization trends in combustion of Chinese oil shale. *Prog. Energ. Combust.*, 2007, **33**(6), 552–579.
9. Loo, L., Konist, A., Neshumayev, D., Pihu, T., Maaten, B., Siirde, A. Ash and flue gas from oil shale oxy-fuel circulating fluidized bed combustion. *Energies*, 2018, **11**(5), 1218.
10. Komaki, A., Goto, T., Uchida, T., Yamada, T., Kiga, T., Spero, C. Operational results of oxyfuel power plant (Callide Oxyfuel Project). *Mechanical Engineering Journal*, 2016, **3**(6), 16-00342.
11. Wu, X. D., Yang, Q., Chen, G. Q., Hayat, T., Alsaedi, A. Progress and prospect of CCS in China: Using learning curve to assess the cost-viability of a 2×600 MW retrofitted oxyfuel power plant as a case study. *Renew. Sust. Energ. Rev.*, 1274–1285.
12. Buhre, B. J. P., Elliot, L. K., Sheng, C. D., Gupta, R. P., Wall, T. F. Oxy-fuel

- combustion technology for coal-fired power generation. *Prog. Energ. Combust.*, 2005, **31**(4), 283–307.
13. Wall, T., Liu, Y. H., Spero, C., Elliott, L., Khare, S., Rathnam, R., Gani, Z. F. A., Moghtaderi, B., Buhre, B., Sheng, C. D., Gupta, R., Yamada, T., Makino, K., Yu, J. L. An overview on oxyfuel coal combustion – State of the art research and technology development. *Chem. Eng. Res. Des.*, 2009, **87**(8), 1003–1016.
 14. Wall, T. F. Combustion processes for carbon capture. *P. Combust. Inst.*, 2007, **31**(1), 31–47.
 15. Zhang, J., Ito, T., Ito, S., Riechelmann, D., Fujimori, T. Numerical investigation of oxy-coal combustion in a large-scale furnace: Non-gray effect of gas and role of particle radiation. *Fuel*, 2015, **139**, 87–93.
 16. Fujimori, T., Yamada, T. Realization of oxyfuel combustion for near zero emission power generation. *P. Combust. Inst.*, 2013, **34**(2), 2111–2130.
 17. Toftegaard, M. B., Brix, J., Jensen, P. A., Glarborg, P., Jensen, A. D. Oxy-fuel combustion of solid fuels. *Prog. Energ. Combust.*, 2010, **36**(5), 581–625.
 18. Gao, H., Runstedtler, A., Majeski, A., Yandon, R., Zanganeh, K., Shafeen, A. Reducing the recycle flue gas rate of an oxy-fuel utility power boiler. *Fuel*, 2015, **140**, 578–589.
 19. Al-Makhadmeh, L., Maier, J., Al-Harabsheh, M., Scheffknecht, G. Oxy-fuel technology: An experimental investigation into oil shale combustion under oxy-fuel conditions. *Fuel*, 2013, **103**, 421–429.
 20. Konist, A., Loo, L., Valtsev, A., Maaten, B., Siirde, A., Neshumayev, D., Pihu, T. Calculation of the amount of Estonian oil shale products from combustion in regular and oxy-fuel mode in a CFB boiler. *Oil Shale*, 2014, **31**(3), 211–224.
 21. Normann, F., Andersson, K., Leckner, B., Johnsson, F. Emission control of nitrogen oxides in the oxy-fuel process. *Prog. Energ. Combust.*, 2009, **35**(5), 385–397.
 22. McCauley, K. J., Farzan, H., Alexander, K. C., McDonald, D. K., Varagani, R., Prabhakar, R., Tranier, J.-P., Perrin, N. Commercialization of oxy-coal combustion: Applying results of a large 30MWth pilot project. *Energy Procedia*, 2009, **1**(1), 439–446.
 23. Rathnam, R. K., Elliott, L. K., Wall, T. F., Liu, Y. H., Moghtaderi, B. Differences in reactivity of pulverised coal in air (O_2/N_2) and oxy-fuel (O_2/CO_2) conditions. *Fuel Process. Technol.*, 2009, **90**(6), 797–802.
 24. Meriste, T., Yörük, C. R., Trikkel, A., Kaljuvee, T., Kuusik, R. TG-FTIR analysis of oxidation kinetics of some solid fuels under oxy-fuel conditions. *J. Therm. Anal. Calorim.*, 2013, **114**(2), 483–489.
 25. Vorres, K. S. The Argonne premium coal sample program. *Energ. Fuel.*, 1990, **4**(5), 420–426.
 26. Cook, E. W. Oil-shale technology in USA. *Fuel*, 1974, **53**(3), 146–151.
 27. Külaots, I., Goldfarb, J. L., Suuberg, E. M. Characterization of Chinese, American and Estonian oil shale semicokes and their sorptive potential. *Fuel*, 2010, **89**(11), 3300–3306.
 28. Williams, P. T., Ahmad, N. Influence of process conditions on the pyrolysis of

- Pakistani oil shales. *Fuel*, 1999, **78**(6), 653–662.
29. Charpenay, S., Serio, M. A., Solomon, P. R. The prediction of coal char reactivity under combustion conditions. *Twenty-Fourth Symposium (International) on Combustion*, 1992, **24**(1), 1189–1197.
 30. Goldfarb, J. L., D’Amico, A., Culin, C., Suuberg, E. M., Kūlaots, I. Oxidation kinetics of oil shale semicokes: Reactivity as a function of pyrolysis temperature and shale origin. *Energ. Fuel.*, 2013, **27**(2), 666–672.
 31. Zaroni, M. A. B., Massard, H., Martins, M. F. Formulating and optimizing a combustion pathways for oil shale and its semi-coke. *Combust. Flame*, 2012, **159**(10), 3224–3234.
 32. Burnham, A. K., Braun, R. L. Global kinetic analysis of complex materials. *Energ. Fuel.*, 1999, **13**(1), 1–22.
 33. Trikkel, A., Kuusik, R., Martins, A., Pihu, T., Stencil, J. M. Utilization of Estonian oil shale semicoke. *Fuel Process. Technol.*, 2008, **89**(8), 756–763.
 34. Senneca, O., Russo, P., Salatino, P., Masi, S. The relevance of thermal annealing to the evolution of coal char gasification reactivity. *Carbon*, 1997, **35**(1), 141–151.
 35. Kūlaots, I., Aarna, I., Callejo, M., Hurt, R. H., Suuberg, E. M. Development of porosity during coal char combustion. *P. Combust. Inst.*, 2002, **29**(1), 495–501.
 36. Zhang, X. J., de Jong, W., Preto, F. Estimating kinetic parameters in TGA using B-spline smoothing and the Friedman method. *Biomass Bioenerg.*, 2009, **33**(10), 1435–1441.

Presented by A. Konist

Received March 14, 2019